Lattice-gas model of nonadditive interacting particles on nanotube bundles

O. A. Pinto, P. M. Pasinetti,[a] F. Nieto, and A. J. Ramirez-Pastor
Departamento de Física, Instituto de Física Aplicada (INFAP), Universidad Nacional de San Luis, CONICET, Chacabuco 917, D5700BWS, San Luis, Argentina

(Received 17 September 2010; accepted 4 December 2010; published online 8 February 2011)

In the present paper, the adsorption thermodynamics of a lattice-gas model which mimics a nanoporous environment is studied by considering nonadditive interactions between the adsorbed particles. It is assumed that the energy linking a certain atom with any of its nearest neighbors strongly depends on the state of occupancy in the first coordination sphere of such an adatom. By means of Monte Carlo (MC) simulations in the grand canonical ensemble, adsorption isotherms and differential heats of adsorption were calculated. Their striking behaviors were analyzed and discussed in terms of the low temperature phases formed in the system. Finally, the results obtained from MC simulations were compared with the corresponding ones from Bragg–Williams approximation. [doi:10.1063/1.3530788]

I. INTRODUCTION

Recently, the advent of modern techniques for building single and multiwalled carbon nanotubes[1–5] has considerably encouraged the investigation of the gas–solid interaction (adsorption and transport of simple and polyatomic adsorbates) in such low-dimensional confining adsorption potentials. The design of carbon tubules as well as of synthetic zeolites and aluminophosphates,[6,7] such as $AlPO_4$-5 having narrow channels, literally provides a way to the experimental realization of quasi-one-dimensional adsorbents. Many studies on conductivity, electronic structure, mechanical strength, etc., of carbon nanotubes are being currently carried out. However, the amount of theoretical and experimental works done on the interaction and thermodynamics of simple gases adsorbed in nanotubes is still limited.

A problem of considerable importance in adsorption is that of determining where on the nanotube bundles the gas molecules adsorb.[8–22] From a theoretical point of view, there are different groups of sites on bundles where the adsorption takes place: (i) the grooves formed between two adjacent tubes on the bundle surfaces, (ii) the interstitial channels formed between the tubes, and (iii) the exterior bundle surface. The access to each group is determined by the size of the adsorbate, the size of the nanotubes forming the bundle, the presence or absence of blocking compounds, etc. Numerous experimental and theoretical studies[8–24] suggest that the admolecules adsorb along the different groups forming one-dimensional systems or lines. There also exists strong evidence of transverse interactions between adjacent lines leading to the formation of ordered phases in the adlayer at low temperature.[19,25]

In this context, many studies have been performed on particular geometries and specific adsorbate–substrate and adsorbate–adsorbate interactions.[16,17,26–29] However, relatively few studies have been undertaken on the general problem of adsorption at critical regime. The present work represents an effort in that direction. Here, a simplified lattice-gas system is studied by Monte Carlo (MC) simulations. The model is an attempt to mimic more general nanoporous environments. Each nanotube has been represented by a one-dimensional chain. These chains were arranged in a triangular cross-sectional structure. We included longitudinal interactions between nearest-neighbor particles adsorbed along a single channel, w^L, and transverse energy between particles adsorbed across nearest-neighbor channels, w^T. Depending on the values of w^L and w^T, different behaviors can be observed.

Previous works[30,31] have been devoted to the case of purely additive (pairwise) interactions. In those studies, different thermodynamic properties such as adsorption isotherms, differential heat of adsorption, and configurational entropy of the adlayer were analyzed. Later, the study of the critical behavior of the system was addressed via MC simulation and finite-size scaling.[32–35]

One way of introducing more complex adsorbate–adsorbate interactions is by considering surface restructuring. In fact, the deviation of an additive behavior appears to be especially significant in the case of chemisorption where the valence electrons are either concentrated in forming a single bond between two isolated atoms or shared among all neighbors which are occasionally occupying sites in the first coordination shell of the central atom.[36–40] Among the effects caused by nonadditive interactions, it is possible to mention the following:[39,40] (i) the symmetry of particle-vacancy (valid for additive interactions) is broken and, consequently, the adsorption thermodynamic quantities (adsorption isotherms, configurational entropy, differential heat of adsorption, etc.) are asymmetric with respect to half coverage; (ii) the formation of "k-mers" (chains of monomers adsorbed on k adjacent lattice sites) is favored at high coverage; (iii) a rich variety of ordered structures are observed in the adlayer; and (iv) for repulsive couplings, first- and second-order phase transitions occur in the adsorbate at different concentrations.

Nonadditive, adsorbate–adsorbate interactions have been recognized in several experimental systems, H on Pd(100), O

[a]Electronic mail: pmp@unsl.edu.ar.

on W(110), and H on Fe(110), just to name a few of them.[41–47] Another evidence of nonadditivity is the tendency to dimer formation. This is observed, for example, in adsorption of Cu and Ni on W(110) for particular coverage values according to thermal desorption spectroscopy analysis.[48] Adsorption of H on graphene (by STM studies) is another example of dimer formation associated with surface restructuring.[49] In the case of adsorption of He on carbon nanotubes, dimer formation has been predicted from studies of diffusion-MC by using Lennard-Jones potentials.[50] There also exists evidence of bundle restructuring (bundle dilation) occurring in adsorption of H_2 in the interstitial channels of nanotube bundles.[51]

The consequences of considering non-pairwise (nonadditive) interactions in the adsorption thermodynamics have been studied for a long time. In fact, statistical mechanics of adsorbed monolayers has been subject of analytical treatment by means of mean field[37,38] and quasichemical[36] approximations. In most of the cited papers, the study has been restricted to some especial cases mainly including attractive interactions. However, the case of repulsive interactions is of interest mainly because (a) experimental phase diagrams corresponding to many systems in the presence of surface restructuring is explained in terms of those interactions;[52–54] (b) the tendency to dimer formation, which it seems to be relevant in several systems mentioned above, can be predicted on the basis of such kind of coupling; and (c) a rich variety of nonsymmetrical phase diagrams (around half coverage) can be described.

In this context, the main aims of the present work are (i) to identify and characterize the most prominent features of the effect of nonadditive repulsive interaction on the thermodynamic quantities describing the adsorption phenomenon on a model of nanopores; (ii) to draw general conclusions on the effect of nonadditive interactions on adsorption; (c) to analyze the results of the simplest theoretical approach, that is, the Bragg–Williams approximation (BWA);[37,38] and (iii) to provide the basis for the evaluation of experimental findings where the nonadditivity is present.

The paper is organized as follows. In Sec. II, the lattice-gas model including nonadditive interactions between adatoms is described. Section III presents the BWA for this model. Section IV shows the results for the adsorption thermodynamics from MC simulations and the comparison with BWA data. Finally, in Sec. V the conclusions and future perspectives are given.

II. MODEL AND BASIC DEFINITIONS

Based on the scheme of a lattice-gas model,[55] an idealized substrate formed by one-dimensional chains with L adsorptive sites is considered.[30–32] These chains were arranged in a triangular structure of size $R \times R$ and periodic boundary conditions in all directions.[30–35] So, a three-dimensional array totaling $M = L \times R \times R$ sites of adsorption is formed, where each site is surrounded by two "axial" sites along the chains and six "transverse" sites belonging to the nearest-neighbor unit cells (see Fig. 1). In order to mimic a nanoporous environment, it seems to be more realistic to consider free boundary

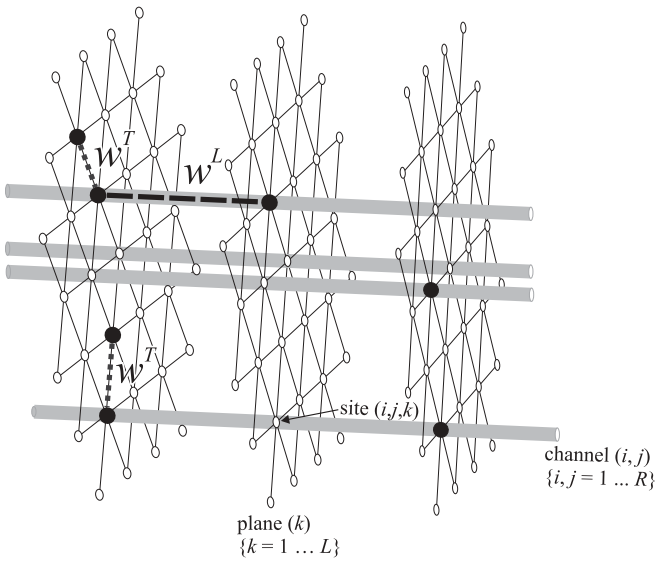

FIG. 1. Schematic representation of the system. Black and white circles correspond to occupied and empty sites, respectively. Dashed (dotted) thick lines represent longitudinal (transverse) lateral interactions.

conditions in the plane $R \times R$. In this sense, it has been proved (this study is not included here for the sake of simplicity) that for the R values of the order of 48 or greater (in the present paper the size R has been set at 60), the equilibrium states of the system do not depend appreciably on the type of boundary conditions used. However, the equilibration time diminishes significantly as periodic boundary conditions are used.

Under these conditions, the Hamiltonian for N monomers adsorbed on M sites can be written as

$$H = \sum_{\langle (i,j,k);(i',j',k)\rangle_T} w^T_{i,j,i',j'} c_{i,j,k} c_{i',j',k} + \sum_{\langle (i,j,k);(i,j,k')\rangle_L} w^L_{k,k'} c_{i,j,k} c_{i,j,k'} - \varepsilon \sum_{(i,j,k)} c_{i,j,k}, \quad (1)$$

where $c_{i,j,k}$ is the local occupation variable which takes the value 1 (0) if the site (i,j,k) is occupied (empty). $w^T_{i,j,i',j'} \equiv w^T$ is the interaction energy between particles on nearest-neighbor transverse sites, while $w^L_{k,k'} \equiv w^L$ is the interaction energy between adjacent occupied axial sites. $\langle (i,j,k);(i',j',k)\rangle_T$ ($\langle (i,j,k);(i,j,k')\rangle_L$) represents pairs of nearest-neighbor transverse (axial) sites and ε corresponds to the interaction energy of a given particle with the substrate (throughout the present paper ε is considered equal to zero without lose of generality). The lateral interaction energies, w^T and w^L, are assumed to depend[30–35] on the occupational states of the surrounding of a given site (i,j,k). The simplest nonadditive dependence for the interaction energy for a given atom and any of its nearest neighbors is to assume that it varies linearly with the number m of them.[36–38] Thus, we have different values for the transverse energies $w^T\{w^T_1, w^T_2, \ldots, w^T_6\}$ and for the axial energies $w^L\{w^L_1, w^L_2\}$, depending on how many first neighbors are actually present in the vicinity of a given atom. Following Ref. 38, we define two nonadditive parameters for the axial and transverse sites separately. The axial nonadditive parameter $P_L w^L_1/w^L_2$ and the

transverse $P_T = w_1^T/w_6^T$ are a measure of the ratio between the strongest and weakest bonds:

$$\frac{w_m^{L(T)}}{w^{L(T)}} = \frac{P_{L(T)}\gamma_{L(T)} - 1}{\gamma_{L(T)} - 1} - m\frac{P_{L(T)} - 1}{\gamma_{L(T)} - 1}, \tag{2}$$

where $\gamma_L = 2$ and $\gamma_T = 6$. When $P_{L(T)} = 1$, the additive case is recovered.[36–40]

The adsorption process is simulated through MC simulations in the grand canonical ensemble.[56–58] We consider the system in contact with an ideal gas at temperature T and chemical potential μ.[39,40] The array as well as the adsorbate are inert upon adsorption. We use the Metropolis scheme[59] to satisfy the principle of detailed balance. A Monte Carlo step (MCs) is achieved when M sites have been tested to change its occupancy state. The thermodynamic equilibrium was achieved after 10^5–10^6 MCs, and then the averages were taken over 10^5–10^6 MCs.

Thermodynamic quantities were calculated as follows:[55]

$$\theta(\mu) = \frac{\langle N\rangle}{M} = \frac{1}{M}\sum_{(i,j,k)}\langle c_{i,j,k}\rangle \qquad \text{(mean coverage)},$$

$$u = \frac{\langle H\rangle - \mu\langle N\rangle}{M} \qquad \text{(mean energy per site)},$$

$$q_d = -\frac{\partial u}{\partial\theta} \qquad \text{(differential heat of adsorption)},$$

where $\langle\cdots\rangle$ denotes the time average over a given number of MCs.

III. BRAGG–WILLIAMS APROXIMATION

In this section, BWA (Refs. 60 and 61) is used for nonadditive interactions.[36–38] The canonical partition function $Q(M,N,T,P_L,P_T)$ for N particles adsorbed on an array of M sites at temperature T and nonadditive lateral interactions is[39,40]

$$Q(N, M, P_L, P_T, T) = \frac{M!}{N!(M-N)!} \times \exp^{-\beta U_{\mathrm{BWA}}(N,M,P_L,P_T)}, \tag{3}$$

where $U_{\mathrm{BWA}}(N, M, P_L, P_T)$ is the mean energy for a system of N particles randomly distributed on M sites, which includes the nonadditive contributions. Now, the energy per site, u_{BWA}, can be defined in terms of the intensive variable θ ($\equiv N/M$):

$$u_{\mathrm{BWA}}(\theta, P_L, P_T) = \frac{U_{\mathrm{BWA}}(N, M, P_L, P_T)}{M} = \frac{\theta}{2}\sum_{m=0}^{\gamma_T} m w_m^T p_{T,m} + \frac{\theta}{2}\sum_{n=0}^{\gamma_L} n w_n^L p_{L,n}. \tag{4}$$

The first (second) term corresponds to transverse (axial) sites. The factor 1/2 is included because each bond is counted twice. Here, P_T,m (p_L,n) is the probability of finding a particle with m (n) first neighbors occupied, and it can be expressed as a function of the mean coverage θ :

$$p_{T,m} = \binom{\gamma_T}{m}\theta^m(1-\theta)^{\gamma_T - m},$$

$$p_{L,n} = \binom{\gamma_L}{n}\theta^n(1-\theta)^{\gamma_L - n}. \tag{5}$$

The combinatorial number corresponds to the degeneracy of the configuration sphere[36,37] and m (n) runs between 0 and 6 (2). Then Eq. (4) becomes

$$u_{\mathrm{BWA}}(\theta, P_L, P_T) = \frac{\theta}{2}\sum_{m=0}^{\gamma_T} m w_m^T \binom{\gamma_T}{m}\theta^m(1-\theta)^{\gamma_T - m} + \frac{\theta}{2}\sum_{n=0}^{\gamma_L} n w_n^L \binom{\gamma_L}{n}\theta^n(1-\theta)^{\gamma_L - n}. \tag{6}$$

By including Eq. (2) in Eq. (6) and after some mathematical manipulations, it results in

$$u_{\mathrm{BWA}}(\theta, P_L, P_T) = \frac{\gamma_T w^T}{2}[P_T\theta^2 + (1-P_T)\theta^3] + \frac{\gamma_L w^L}{2}[P_L\theta^2 + (1-P_L)\theta^3]. \tag{7}$$

Then, the Helmholtz free energy per site, f, being $\beta f = -(1/M)\ln Q$, can be written as[60,61]

$$\beta f(\theta, T, P_L, P_T) = \theta\ln\theta - (1-\theta)\ln(1-\theta) + \frac{\beta\gamma_T w^T}{2}[P_T\theta^2 + (1-P_T)\theta^3] + \frac{\beta\gamma_L w^L}{2}[P_L\theta^2 + (1-P_L)\theta^3]. \tag{8}$$

Finally, the adsorption isotherm can be expressed as[60]

$$\beta\mu = -\left[\frac{\partial(\beta f)}{\partial\theta}\right]_T = \ln\left[\frac{\theta}{1-\theta}\right] + \frac{\beta\gamma_T w^T}{2}[2P_T\theta + 3(1-P_T)\theta^2] + \frac{\beta\gamma_L w^L}{2}[2P_L\theta + 3(1-P_L)\theta^2]. \tag{9}$$

Note that whether $P_L = P_T = 1.0$, $\gamma_L = 2$, and $\gamma_T = 6$, Eqs. (7)–(9) recover the additive form given in Ref. 33. On the other hand, by taking $w^L = 0$, Eqs. (7)–(9) correspond to the expressions published by Milchev and Paunov[37] for a two-dimensional system.

IV. RESULTS

MC simulations have been performed in a lattice of size $L = 96$ and $R = 60$. Repulsive interactions have been considered for all the cases studied (for simplicity, we take $w^T = w^L = \mathrm{w} = 1$).

Case I: $P_T = 1.0$, $P_L \neq 1.0$,

Case II: $P_T \neq 1.0$, $P_L = 1.0$,

Case III: $P_T \neq 1.0$, $P_L \neq 1.0$.

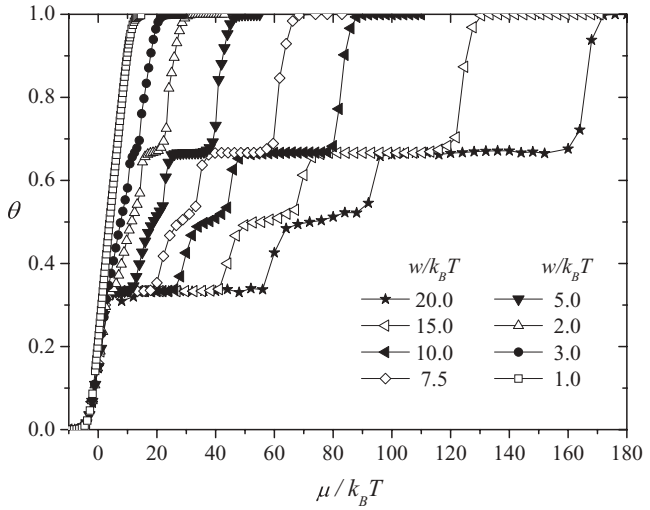

FIG. 2. Adsorption isotherms for $P_T = 1.0$ and $P_L = 0.7$ and several values of temperature.

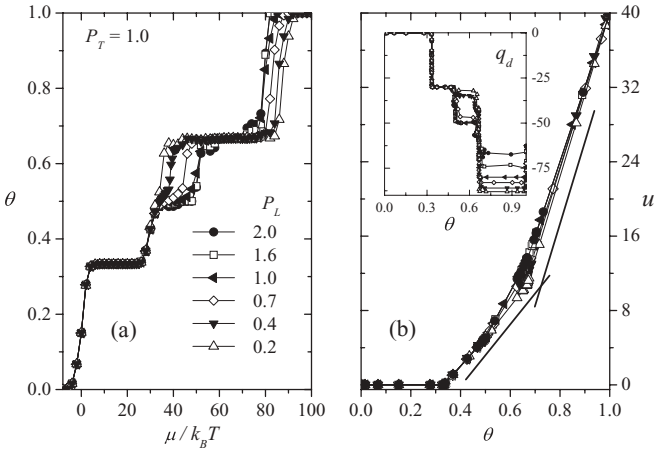

FIG. 3. (a) Adsorption isotherms for $w/k_BT = 10.0$, $P_T = 1.0$, and several values of P_L as indicated. (b) Energy per site, u, vs coverage for the same values of P_L and P_T. The solid lines are a guide to the eyes. The inset shows the corresponding curves of the differential heat of adsorption, q_d.

Case I is analyzed in Figs. 2 and 3. In the former, adsorption isotherms are shown for $P_T = 1.0$, $P_L = 0.7$, and different values of w/k_BT as indicated. As it is expected, the isotherms recover the Langmuir case (lattice-gas without lateral interactions) in the high temperature regime.

For low temperature (lower than the critical one) the same three plateaus as in the additive case are observed.[31] The plateaus, at coverage $\theta = 1/3$ and $\theta = 2/3$, correspond to the formation of the well-known $(\sqrt{3} \times \sqrt{3})$ and $(\sqrt{3} \times \sqrt{3})$* ordered phases in the planes, respectively. In addition, given that $w^L > 0$, particles avoiding configurations with nearest-neighbor axial interactions develop a structure of alternating particles along the channels (each successive plane is obtained from the previous one under simultaneous inversion of all the occupational values). The plateau at $\theta = 1/2$ correspond to a partially ordered structure, where each particle is surrounded by two nearest neighbors in the transverse direction (same plane).

In this framework, the presence of nonadditive interactions along the channels, particularly the case $P_L < 1$, privileges the coupling of particles surrounded by one nearest neighbor [$w_2^L < w_2^L$, see Eq. (2)], favoring the formation of dimers in the axial direction. Consequently, the $(\sqrt{3} \times \sqrt{3})$* ordered phase is reinforced (the plateau at $\theta = 2/3$ is wider than the corresponding one at $\theta = 1/3$), and the symmetry of particle-vacancy with respect to $\theta = 1/2$ is broken.

In Figs. 3(a) and 3(b), respectively, adsorption isotherms and energy of adsorption per site are presented for $w/k_BT = 10$, $P_T = 1.0$, and several values of P_L. From a simple inspection of the figure, different adsorption regimes are observed. In the range of coverage between $0 < \theta \leq 1/3$, the lattice sites are filled until the $(\sqrt{3} \times \sqrt{3})$ structure is formed. Upon increasing the surface coverage, a plateau is observed at $\theta = 1/2$ as it was previously described[31] for $P_L = 1.0$. This plateau, due to particles avoiding configurations with nearest-neighbor axial interactions, develops a structure of alternating particles along the channels. This effect is reinforced for $P_L > 1.0$ because w_2^L increases with respect to w_2^L. On the contrary, as it was discussed above, if $P_L < 1.0$ (and w_2^L decreases with respect to w_2^L) the particles interact in such a way that the formation of dimers along the channels is favored and consequently the plateau at $\theta = 1/2$ tends to disappear. Thus, at $P_L = 0.2$, this plateau is completely absent.

The previous arguments justify the existence of a plateau at $\theta = 2/3$, which becomes broader as P_L decreases. In this case, there is one axial interaction per particle in the $(\sqrt{3} \times \sqrt{3})$* structure ($w_1^L < w_2^L$ for $P_L < 1.0$), and the filling of the channels consists of pairs of particles separated by one

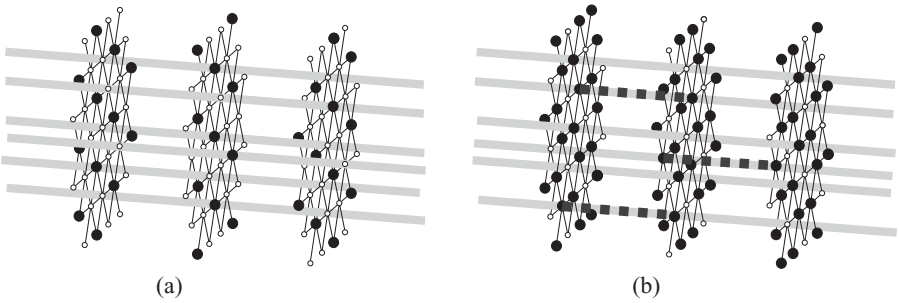

FIG. 4. Schematic representations of the adlayer for $P_T = 1$ and $P_L < 1$. (a) At coverage $\theta = 1/3$, the $(\sqrt{3} \times \sqrt{3})$ ordered phase is formed in each plane and successive planes are formed avoiding longitudinal interactions. (b) At coverage $\theta = 2/3$, the $(\sqrt{3} \times \sqrt{3})$* ordered phase is formed in each plane. The dotted segments indicate the "dimerlike" structure along the channels.

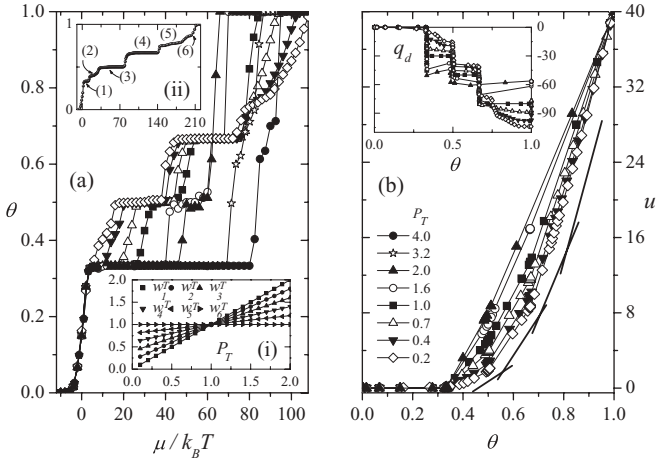

FIG. 5. (a) Adsorption isotherms for $w/k_BT = 10.0$, $P_L = 1.0$, and several values of P_T as indicated. Inset (i) shows the dependence of w_m^T on P_T. In inset (ii), the adsorption isotherm at the lowest temperature considered here, $w/k_BT = 20.0$, is shown. It is possible to identify the different plateaus at $\theta = 1/3$, 2/5, 2/3, 3/4, and 6/7. (b) Energy per site vs coverage. The curves correspond to the same cases showed in part (a) (the solid lines are a guide to the eyes). The inset shows the differential heat of adsorption, q_d.

empty site (dimerlike structure). Figures 4(a) and 4(b) show the structures formed in this case. For $P_L > 1.0$ (and $\theta = 2/3$) the situation is quite different: there are two axial interactions per particle, and the $(\sqrt{3} \times \sqrt{3})^*$ structure propagates in all planes. This configuration has no effect on the plateaus, and there is no appreciable difference with the additive case ($P_L = 1$).

The plateaus in the adsorption isotherms, which are clearly associated with different structural rearrangements of the adsorbed particles, are accompanied by characteristic signals in the energy of adsorption and the differential heat of adsorption. In fact, a plateau in the isotherms appears as both a change in the slope of the energy of adsorption and a step in the differential heat of adsorption. This behavior is shown in part (b) of Fig. 3 and its corresponding inset, confirming the discussion of part (a).

For Case II, the adsorption isotherms at $w/k_BT = 10.0$ are presented in part (b) of Fig. 5, where three plateaus at the critical densities $\theta = 1/3$, 1/2, and 2/3 are shown. Different situations can be considered according to the value of P_T. Namely, for $P_T > 1$, w_l^T is larger than w_m^T ($m = 2,\ldots,6$) [see inset (i) in Fig. 5(a)]. Consequently, the particles avoid to be coupled in the plane, and while the plateaus at $\theta = 1/2$ and $\theta = 2/3$ diminish, the width of the plateau at $\theta = 1/3$ is increased. For the extreme values of P_T ($P_T \geq 2$), the plateaus at $\theta = 1/2$ and $\theta = 2/3$ disappear and the isotherms exhibit discontinuities, i.e., jumps in the surface coverage, from $\theta = 1/3$ ($\theta = 1/2$) to $\theta = 1/2$ (full coverage), which could be an indication of a first-order phase transition. The system prefers condensate instead of any sequential filling.

On the contrary, for $P_T < 1$, w_l^T is smaller than w_m^T ($m = 2,\ldots,6$) [see inset (i) in Fig. 5(a)], and the plateaus at $\theta = 1/2$ and $\theta = 2/3$ are reinforced while the plateau at $\theta = 1/3$ diminishes. In the limit of $P_T = 0.2$, the $(\sqrt{3} \times \sqrt{3})$ ordered phase tends to disappear. The isotherm for $w/k_BT = 20.0$ and $P_T = 0.2$ is shown in inset (ii) of Fig. 5(a). Three new plateaus at $\theta = 2/5$, 3/4, and 6/7 can be identified. In order to clarify the situation, each plateau has been labeled with a number in the rising order of appearance from 1 to 6. The additional ordered structures that appear in the transverse planes are shown in Fig. 6. The behavior of the curves and the corresponding structures have already been reported in Ref. 40 for a two-dimensional system. This finding is not surprising, because the only effect of the longitudinal repulsive interactions is to

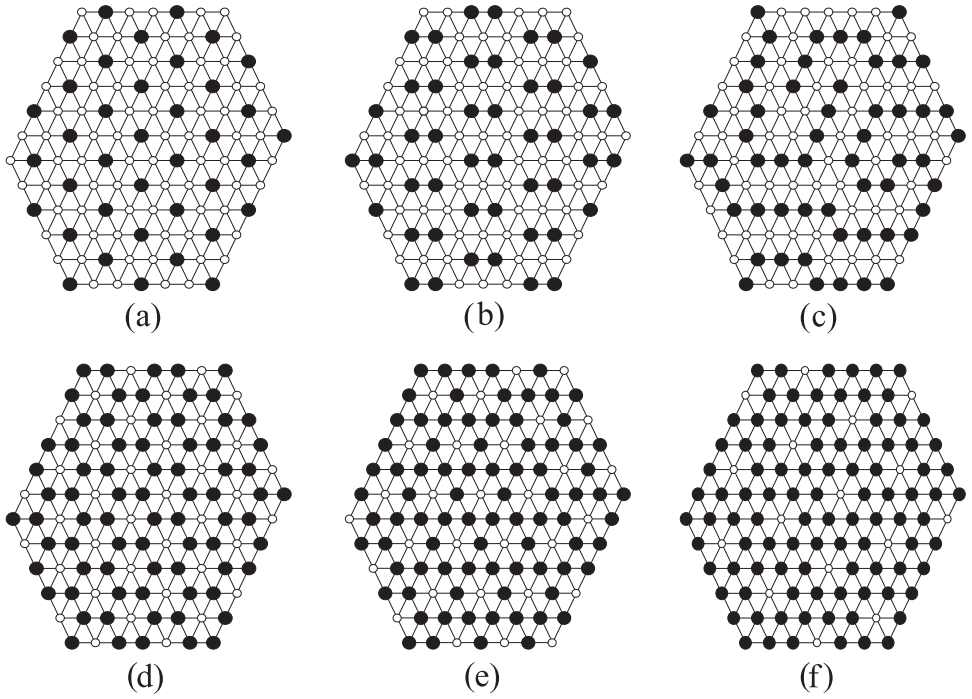

FIG. 6. Typical snapshots of a transverse plane showing the various low temperature ordered structures for $P_T = 1$ and $P_L = 0.2$. (a) $\theta = 1/3$, (b) $\theta = 2/5$, (c) $\theta = 1/2$, (d) $\theta = 2/3$, (e) $\theta = 3/4$, and (f) $\theta = 6/7$. The longitudinal order (if any) is explained in the text.

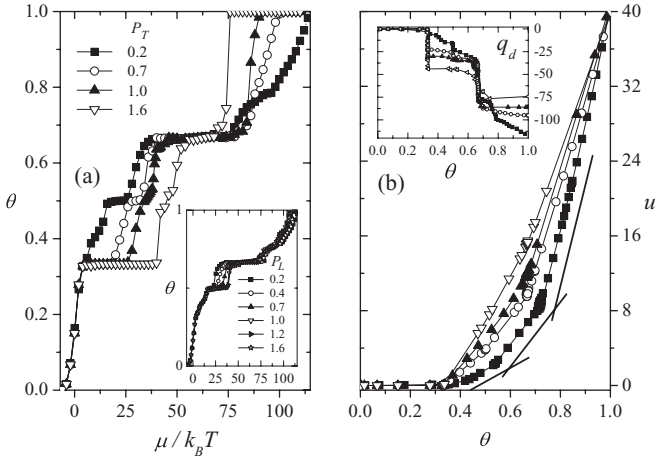

FIG. 7. (a) Adsorption isotherms for $w/k_BT = 10.0$, $P_L = 0.4$, and several values of P_T as indicated. In the inset, the case of $w/k_BT = 10.0$, $P_T = 0.2$, and different values of P_L as indicated is shown. (b) Energy per site, u, vs coverage for the same values of nonadditivity as in part (a). The solid lines are a guide to the eyes. The inset shows the differential heat of adsorption, q_d.

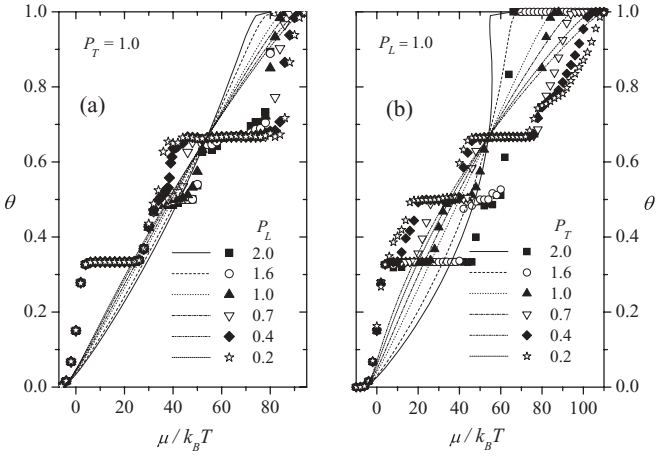

FIG. 8. Comparison between the results from MC (symbols) and BWA (lines). Adsorption isotherms at $w/k_BT = 10.0$ for (a) Case I and (b) Case II.

avoid the formation of occupied–occupied pairs of sites along the channels.

In Fig. 5(b), the energy per site and the differential heat of adsorption are plotted in the main framework and in the inset, respectively. Both quantities support the observations already obtained from the isotherms. Again, the breaking of the vacancy-particle symmetry is observed in the shape of all curves ($P_T > 1$ and $P_T < 1$).

In order to complete the analysis, in Case III we have considered the simultaneous effect of nonadditivity in both longitudinal and transverse directions. The behavior of the system can be understood as a combination of the first two cases.

The adsorption isotherms for $w/k_BT = 10.0$, $P_L = 0.4$, and several values of P_T are shown in Fig. 7(a). The figure shows four plateaus at $\theta = 1/3$, 1/2, 2/3, and 3/4, respectively. These plateaus correspond to the ordered structures identified in Case II (the plateaus at $\theta = 2/5$ and $\theta = 6/7$ are not present for $w/k_BT = 10.0$). At $P_T = 1.6$, the plateaus are narrow at $\theta = 1/2$ and $\theta = 2/3$, and an abrupt jump from $\theta = 2/3$ to full coverage is observed. In the inset of Fig. 7(a), the isotherms for $w/k_BT = 10.0$, $P_T = 0.2$, and different values of P_L are shown. In the case of $P_L > 1.0$, it is possible to observe plateaus at $\theta = 3/4$ and $\theta = 6/7$, which were already observed in Case II. Here, the main influence of the longitudinal parameter is to weaken (strengthen) the ordered structure at $\theta = 1/2$ ($\theta = 2/3$) for $P_L < 1$ ($P_L > 1$). In Fig. 7(b), the energy per site and the differential heat are shown.

Now, we shall compare the MC simulation data with BWA results. Figures. 8(a) and 8(b) show the isotherms for MC simulations (symbols) and the theoretical approximation (lines). BWA does not predict any plateaus. For $P_T = 2.0$ [Fig. 8(b)], the theoretical approach presents a typical van der Waals loop in agreement with the jump in the MC results. The approximation predicts the condensation similar to what happens in the first-order phase transition.

In order to quantify the difference between simulation and theoretical results, the absolute error, $E_R(\theta)$, is defined as[33]

$$E_R(\theta) = |\beta\mu_{\mathrm{BWA}}(\theta) - \beta\mu_{\mathrm{MC}}(\theta)|, \tag{10}$$

where μ_{BWA} (μ_{MC}) is the chemical potential obtained from BWA (MC simulations) for a fixed value of θ. The errors are shown in Figs. 9(a) and 9(b). As can be seen, BWA represents better simulation for the range of coverage between 1/3 and 2/3. For studying the errors in the complete range of coverage, we can define the integral error, E_I, as

$$E_I = \int_0^1 E_R(\theta)\, d\theta. \tag{11}$$

The integral errors are shown in the insets of Fig. 9. For this analysis, the minima errors are found for the values of P_L and P_T close to the additive case. Finally, one can expect that this degree of approximation (BWA) improves to higher temperatures in all cases. The explanation of this effect is simple: the main assumption of BWA says that the configurational

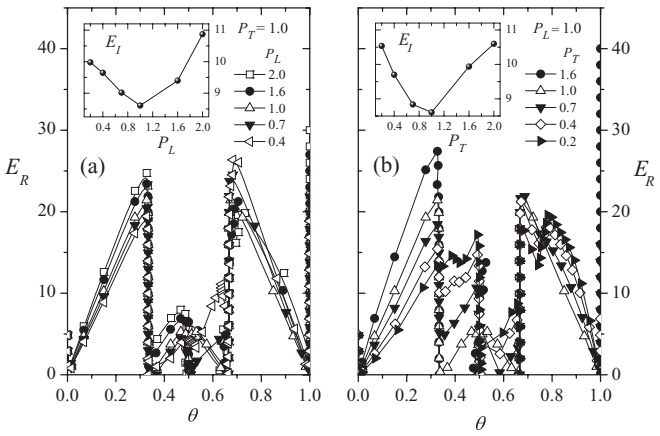

FIG. 9. Absolute error (in k_BT units), E_R, vs surface coverage for the adsorption isotherms at $w/k_BT = 10.0$ corresponding to (a) Case I and (b) Case II. The insets show the integral errors, E_I, vs the corresponding nonadditive parameter.

degeneracy and the average nearest-neighbor interaction energy are treated as though the molecules were distributed randomly among the sites. In other words, all configurations of N particles on M sites have the same weight as they would have $w/k_BT = 0$ (or $T \to \infty$). This is obviously an incorrect procedure when an ordered structure is formed on the surface.

To conclude, it is important to note that the critical behavior (ordered phases and nature of the phase transitions) observed in the present study would remain the same for systems with $L \to \infty$ and R in the order of 48 or greater. For smaller R (and free boundary conditions), different structures are expected to appear in the adlayer, depending on each particular value of R. A detailed discussion on this point is out of the scope of this paper and will be the object of future work.

V. CONCLUSIONS

In the present work, the main adsorption properties of a system of monomers on a low-dimensional system, considering nonadditive interactions between particles have been addressed. The study was carried out through MC simulations in the grand canonical ensemble and BWA. A lattice-gas model was used for describing the system where each nanotube or unit cell was represented by a one-dimensional array. These channels were arranged in a triangular cross-sectional structure. We introduced the nonadditivity independently for the longitudinal and transverse directions via two parameters, P_L and P_T, respectively. Depending on the values of those parameters, different behaviors in adsorption isotherms, energy per site, and differential heat of adsorption were found:

1. For the so named Case I, where only longitudinal nonadditive interaction was considered, we found the formation of ordered phases in the transverse planes. For $P_L < 1.0$, the longitudinal interactions reinforce the $(\sqrt{3} \times \sqrt{3})^*$ ordered phase at the expense of a weakening of the plateau at $\theta = 1/2$. For $P_L > 1$, the situation is the opposite. It is possible to think these findings to be a consequence of the dimer formation in the longitudinal directions, which is a direct effect of the presence of nonadditive interactions. In fact, the $(\sqrt{3} \times \sqrt{3})^*$ ordered phase is reinforced (the plateau at $\theta = 2/3$ is wider than the corresponding one at $\theta = 1/3$). The breaking of the particle-vacancy symmetry with respect to $\theta = 1/2$ and the continuous feature of the phase transitions involved in the process are evident. There are no new phases as compared with the additive case.
2. When only transverse nonadditive interactions were considered (Case II), a rich variety of low temperature ordered phases are observed in the system. In this case, new ordered phases appear as compared with the additive case, and by depending on the values of P_T, either the system goes through a continuous phase transition or the isotherms exhibit discontinuities which could be interpreted as a first-order phase transition. Here, the formation of dimers occurs in the transverse planes, which, as in Case I, is a direct effect of the presence of nonadditive interactions. Again, the broken of the vacancy-particle symmetry is observed in the shape of all curves ($P_T > 1$ and $P_T < 1$).
3. If we consider nonadditivity in both directions (Case III), the situation can be described as a combination of the previously analyzed cases.
4. The analytical approach does not reproduce the simulation results for high values of lateral interactions. However, at $P_T > 1.0$ ($P_L = 1$), the approximation presents a van der Waals loop, in agreement with the jump in the MC results. The errors show that BWA performs better for values of the nonadditive parameters close to unity.

ACKNOWLEDGMENTS

This work was supported in part by CONICET (Argentina) under Project No. PIP 112-200801-01332, Universidad Nacional de San Luis (Argentina) under Project No. 322000, and the National Agency of Scientific and Technological Promotion (Argentina) under Project No. 33328 PICT 2005. All calculations were carried out using the BACO2 parallel cluster (composed by 60 PCs each with a 3.0 GHz Pentium-4 processor and 60 PCs each with a 2.4 GHz Core 2 Quad processor) located at Instituto de Física Aplicada (INFAP), CONICET, Universidad Nacional de San Luis, San Luis, Argentina.

[1] S. Iijima, Nature (London) **354**, 56 (1991).
[2] S. Iijima and T. Ichihashi, Nature (London) **363**, 603 (1993).
[3] D. S. Bethune, C. H. Kiamg, M. S. deVries, G. Gorman, R. Savoy, J. Vasquez, and R. Beyers, Nature (London) **363**, 605 (1993).
[4] P. M. Ajayan and S. Iijima, Nature (London) **361**, 333 (1993).
[5] E. Dujardin, T. W. Ebbesen, H. Hiura, and K. Tanigaki, Science **265**, 1850 (1994).
[6] C. Martin, J. P. Coulomb, Y. Grillet, and R. Kahn, in *Fundamentals of Adsorption: Proceedings of the Fifth International Conference*, edited by M. D. LeVan (Kluwer Academic, Boston, MA, 1996), p. 587.
[7] C. Martin, N. Tosi-Pellenq, J. Patarin, and J. P. Coulomb, Langmuir **14**, 1774 (1998).
[8] A. D. Migone and S. Talapatra, in *Encyclopedia of Nanoscience and Nanotechnology*, edited by H. S. Nalwa (American Scientific, Los Angeles, CA, 2004), Vol. 4, p. 749.
[9] G. Stan, M. J. Bojan, S. Curtarolo, S. M. Gatica, and M. W. Cole, Phys. Rev. B **62**, 2173 (2000).
[10] T. Wilson, A. Tyburski, M. R. DePies, O. E. Vilches, D. Becquet, and M. Bienfait, J. Low Temp. Phys. **126**, 403 (2002).
[11] T. Wilson and O. E. Vilches, Low Temp. Phys. **29**, 732 (2003).
[12] N. M. Urban, S. M. Gatica, M. W. Cole, and J. L. Riccardo, Phys. Rev. B **71**, 245410 (2005).
[13] M. Bienfait, P. Zeppenfeld, N. Dupont-Pavlovsky, M. Muris, M. R. Johnson, T. Wilson, M. DePies, and O. E. Vilches, Phys. Rev. B **70**, 035410 (2004).
[14] M. M. Calbi, S. M. Gatica, M. J. Bojan, G. Stan, and M. W. Cole, Rev. Mod. Phys. **73**, 857 (2001).
[15] M. M. Calbi and J. L. Riccardo, Phys. Rev. Lett. **94**, 246103 (2005).
[16] R. A. Trasca, M. M. Calbi, and M. W. Cole, Phys. Rev. E **65**, 061607 (2002).
[17] R. A. Trasca, M. M. Calbi, M. W. Cole, and J. L. Riccardo, Phys. Rev. E **69**, 011605 (2004).
[18] L. Chen and J. K. Johnson, Phys. Rev. Lett. **94**, 125701 (2005).
[19] J. V. Pearce, M. A. Adams, O. E. Vilches, M. R. Johnson, and H. R. Glyde, Phys. Rev. Lett. **95**, 185302 (2005).
[20] L. Heroux, V. Krungleviciute, M. M. Calbi, and A. D. Migone, J. Phys. Chem. B **110**, 1297 (2006).
[21] S. M. Gatica, M. J. Bojan, G. Stan, and M. W. Cole, J. Chem. Phys. **114**, 3765 (2001).
[22] W. Shi and K. J. Johnson, Phys. Rev. Lett. **91**, 015504 (2003).

[23]A. Kuznetsova, J. T. Yates, Jr., J. Liu, and R. E. Smalley, J. Chem. Phys. **112**, 9590 (2000).
[24]A. Kuznetsova, D. B. Mawhinney, V. Naumenko, J. T. Yates, Jr., J. Liu, and R. E. Smalley, Chem. Phys. Lett. **321**, 292 (2000).
[25]M. W. Cole, V. H. Crespi, G. Stan, C. Ebner, J. M. Hartman, S. Moroni, and M. Boninsegni, Phys. Rev. Lett. **84**, 3883 (2000).
[26]Lev D. Gelb, K. E. Gubbins, R. Radhakrishnan, and M. Sliwinska-Bartkowiak, Rep. Prog. Phys. **62**, 1753 (1999).
[27]A. J. Ramirez-Pastor, T. P. Eggarter, V. D. Pereyra, and J. L. Riccardo, Phys. Rev. B **59**, 11027 (1999).
[28]A. J. Ramirez-Pastor, A. Aligia, F. Romá, and J. L. Riccardo, Langmuir **16**, 5100 (2000).
[29]F. Romá and A. J. Ramirez-Pastor, Phys. Rev. E **69**, 036124 (2004).
[30]P. M. Pasinetti, J. L. Riccardo, and A. J. Ramirez-Pastor, J. Chem. Phys. **122**, 154708 (2005).
[31]P. M. Pasinetti, J. L. Riccardo, and A. J. Ramirez-Pastor, Physica A **355**, 383 (2005).
[32]P. M. Pasinetti, F. Roma, J. L. Riccardo, and A. J. Ramirez-Pastor, J. Chem. Phys. **125**, 214705 (2006).
[33]M. Dávila, P. M. Pasinetti, F. Nieto, and A. J. Ramirez-Pastor, Physica A **385**, 221 (2007).
[34]P. M. Pasinetti, F. Roma, J. L. Riccardo, and A. J. Ramirez-Pastor, Solid State Phenom. **150**, 73 (2009).
[35]P. M. Pasinetti, F. Romá, J. L. Riccardo, and A. J. Ramirez-Pastor, J. Chem. Phys. **132**, 054111 (2010).
[36]A. Milchev, J. Chem. Phys. **78**, 1994 (1983).
[37]A. Milchevand and M. Paunov, Surf. Sci. **108**, 25 (1981).
[38]A. Milchev and K. Binder, Surf. Sci. **164**, 1 (1985).
[39]O. A. Pinto, A. J. Ramirez-Pastor, and F. Nieto, Surf. Sci **602**, 1763 (2008).
[40]O. A Pinto, A. J. Ramirez-Pastor, and F. Nieto, Physica A **389**, 3456 (2010).
[41]W. H. Ching, D. Huber, M. G. Lagally, and G.-C. Wang, Surf. Sci. **77**, L497 (1979).
[42]R. Imbihl, R. J. Behm, K. Chritmann, G. Ertl, and T. Matsushima, Surf. Sci. **117**, 257 (1982).
[43]K. Binder and D. P. Landau, Surf. Sci. **108**, 503 (1981).
[44]L. C. A. Stoop, Thin Solid Films **103**, 375 (1983).
[45]K. Kaski, W. Kinzel, and J. D. Gunton, Phys. Rev. B **27**, 6777 (1983).
[46]P. A. Rikvold, K. Kaski, J. D. Gunton, and M. C. Yalabik, Phys. Rev. B **29**, 6285 (1984).
[47]F. H. Ree and C. F. Bender, Phys. Rev. Lett. **32**, 85 (1974).
[48]J. Kolaczkiewicz and E. Bauer, Surf. Sci. **151**, 333 (1985).
[49]R. Balog, B. Jørgensen, J. Wells, E. Lægsgaard, P. Hofmann, F. Besenbacher, and L. Hornekær J. Am. Chem. Soc. **131**, 8744 (2009).
[50]D. Hirashima and K. Yamashita, J. Low Temp. Phys. **158**, 112 (2010).
[51]M. C. Gordillo, J. Boronat, and J. Casulleras, Phys. Rev. B **68**, 1254211 (2003).
[52]T. E. Felter and P. J. Estrup, Phys. Rev. Lett. **38**, 1138 (1977).
[53]F. Nieto and V. Pereyra, Surf. Sci. **383**, 308 (1997).
[54]F. Nieto and V. Pereyra, Surf. Sci. **399**, 96 (1998).
[55]G. Zgrablich, in *Equilibria and Dynamics of Gas Adsorption on Heterogeneous Solid Surfaces*, edited by W. Rudzinski and G. Zgrablich (Elsevier, Amsterdam, 1996).
[56]D. Nicholson, N. D. Parsonage, *Computer Simulation and the Statistical Mechanics of Adsorption* (Academic, London, 1982).
[57]*Monte Carlo Methods in Statistical Physics*, 2nd ed, edited by K. Binder (Springer-Verlag, Berlin, 1986).
[58]*Applications of the Monte Carlo Method in Statistical Physics*, edited by K. Binder (Springer-Verlag, Berlin, 1984).
[59]N. Metrópolis and S. Ullam, J. Am Stat. Assoc. **44**, 335 (1949).
[60]T. L. Hill, *An Introduction to Statistical Thermodynamics* (Addison-Wesley, Reading, MA, 1960).
[61]K. Huang, *Statistical Mechanics* (Wiley, New York, 1963).